

REALISTIC INTERACTIONS AND CONFIGURATION MIXING IN FERMIONIC MOLECULAR DYNAMICS

T. NEFF, H. FELDMEIER and R. ROTH

*Gesellschaft für Schwerionenforschung mbH
Planckstraße 1, D-64291 Darmstadt, Germany*

J. SCHNACK

*Universität Osnabrück, Fachbereich Physik
Barbarastraße 7, D-49069 Osnabrück, Germany*

Abstract

In Fermionic Molecular Dynamics the occurrence of multifragmentation depends strongly on the intrinsic structure of the many-body state. Slater determinants with narrow single-particle states and a cluster substructure show multifragmentation in heavy-ion collisions while those with broad wave functions, which resemble more a shell-model picture, deexcite by particle emission. Which of the two type of states occurs as the ground state minimum or as a local minimum in the energy depends on the effective interaction. Both may equally well reproduce binding energy and radii of nuclei. This ambiguity led us to reinvestigate the derivation of the effective interaction from realistic nucleon-nucleon potentials by means of a unitary correlation operator which is much more suited for dynamical calculations than the G-matrix or the Jastrow method. First results of mixing many Slater determinants are also presented.

1 Fermionic Molecular Dynamics

Fermionic Molecular Dynamics (FMD) [2, 3, 5] is a model to describe ground states of atomic nuclei and heavy-ion reactions in the low to medium energy regime below the threshold for particle production.

The FMD trial state $|\hat{Q}\rangle$ takes care of the Pauli principle explicitly by using a Slater determinant of gaussian single-particle states $|q_i\rangle$.

$$|\hat{Q}\rangle = \tilde{C}\tilde{\mathcal{A}}(|q_1\rangle \otimes \cdots \otimes |q_A\rangle) \quad (1)$$

$\tilde{\mathcal{A}}$ is the antisymmetrization operator and \tilde{C} is an optional unitary correlation operator which will be discussed later.

The single-particle states $|q_i\rangle$ are gaussians with mean position and mean momentum parametrized by 3 complex parameters \vec{b} and a dynamical complex width a . Spin $|\chi\rangle$ and isospin $|\xi\rangle$ are usually parametrized as two-spinors

$$\langle \vec{x} | q \rangle = \langle \vec{x} | a, \vec{b}, \chi, \xi \rangle = \exp\left\{-\frac{(\vec{x}-\vec{b})^2}{2a}\right\} |\chi\rangle \otimes |\xi\rangle. \quad (2)$$

The description with gaussian single-particle states is the closest analogue to a classical phase-space trajectory and therefore allows for a descriptive interpretation of the FMD time evolution. The gaussians form an overcomplete set and allow to represent shell-model states as well as intrinsically deformed states.

The dynamical equations are derived from the time-dependent variational principle

$$\delta \int dt \frac{\langle \hat{Q} | i \frac{d}{dt} - \tilde{H} | \hat{Q} \rangle}{\langle \hat{Q} | \hat{Q} \rangle} = 0. \quad (3)$$

The variation with respect to the parameters q_ν which are contained in the trial state $|\hat{Q}\rangle$ leads to the Euler-Lagrange equations of motion

$$i \sum_{\nu} \mathcal{C}_{\mu\nu} \dot{q}_{\nu} = \frac{\partial \mathcal{H}}{\partial q_{\mu}^*} \quad (4)$$

with generalized forces given by the gradient of the Hamilton function \mathcal{H} and the matrix \mathcal{C} which describes the geometrical structure of the fermion phase-space.

$$\mathcal{C}_{\mu\nu} = \frac{\partial}{\partial q_{\mu}^*} \frac{\partial}{\partial q_{\nu}} \ln \langle \hat{Q} | \hat{Q} \rangle, \quad \mathcal{H} = \frac{\langle \hat{Q} | \tilde{H} | \hat{Q} \rangle}{\langle \hat{Q} | \hat{Q} \rangle} \quad (5)$$

The initial state of a reaction, which is evolved in time according to eq. (4), is the antisymmetrized product of boosted ground states.

2 Multifragmentation

The results of FMD calculations for multifragmentation reactions show a strong dependence on the intrinsic structure of the nuclear states which is determined by the effective interaction. All nucleon-nucleon interactions which we use are adjusted to describe well binding energies and radii of ground states. They differ mainly in their momentum dependent parts which are poorly determined by the ground state properties but can lead to very different behavior in the dynamics of a heavy-ion reaction. This effect is demonstrated in fig. 1 where we display density contour plots of $^{40}\text{Ca}+^{40}\text{Ca}$ reactions at energy $E_{lab} = 35 \text{ A MeV}$ and impact parameter $b = 2.75 \text{ fm}$.

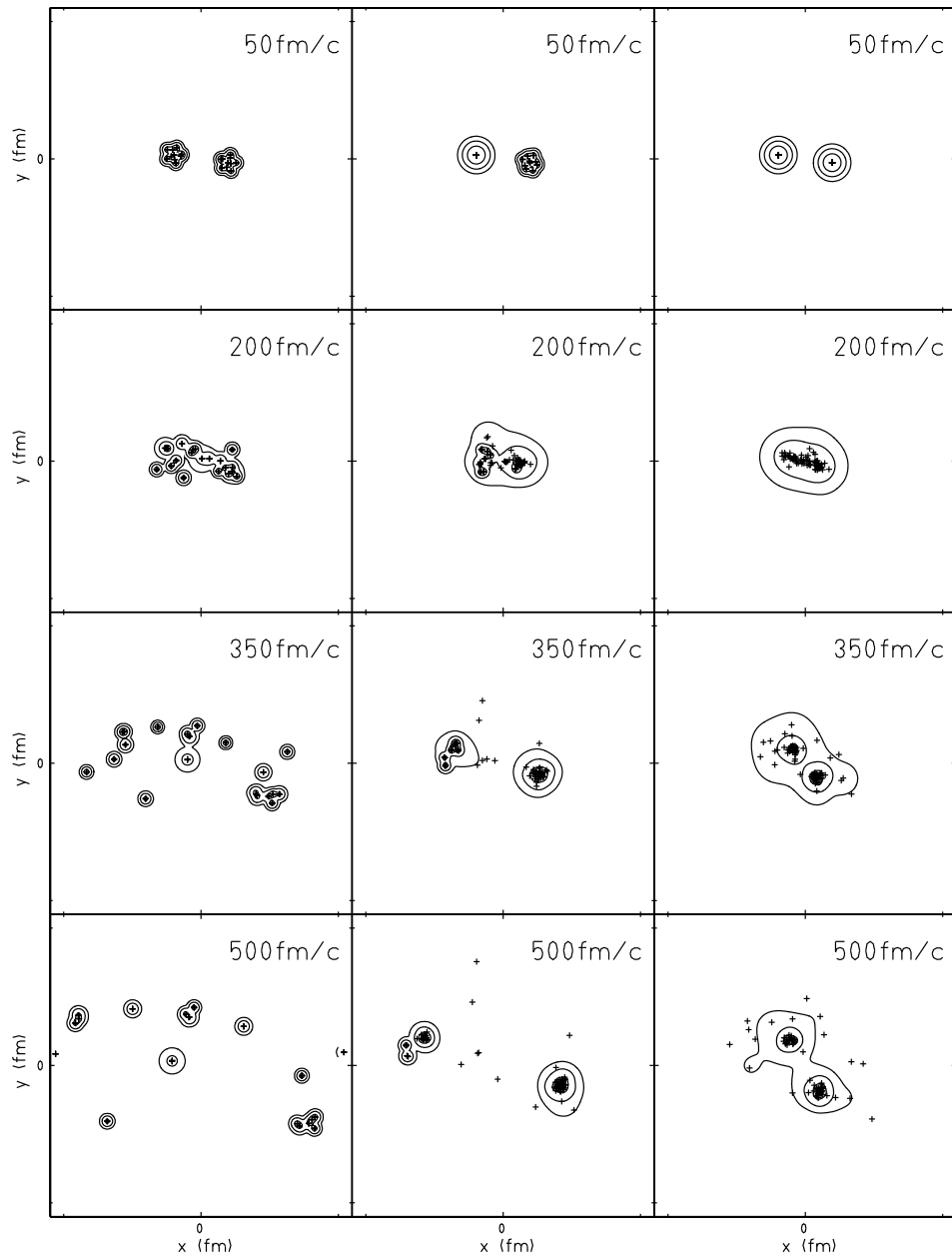


Figure 1: Density plots of $^{40}\text{Ca}+^{40}\text{Ca}$ at $E_{lab} = 35 \text{ A MeV}$ and $b = 2.75 \text{ fm}$. Crosses indicate centroids of gaussians. Crosses without surrounding contours are from wave packets which have spread so much that their density is below the lowest contour (evaporated nucleon).

The used phenomenological interaction has an FMD ground state with an α -cluster structure. Only 1 MeV above is a stationary FMD state (local minimum) which shows no clustering in coordinate space but looks more like a closed spherical sd-shell nucleus. These two energetically almost degenerate states behave completely different in heavy ion reactions. The clustered states lead to multifragmentation where the spatial correlations in the initial state survive to a large extent the collision. Reactions with the spherical states show no multifragmentation. Here we observe binary inelastic collisions followed by deexcitation through evaporation of single nucleons. Collisions between the two different types of FMD states result in a somewhat mixed situation. It also happens that a smooth nucleus sometimes jumps during a collision into a cluster configuration and vice-versa.

The effect of initial correlations is further studied in the decay of excited ^{56}Fe nuclei where the initial excitation energy was created in different ways. In the upper rows of fig. 2 we can see the effect of random excitations which destroy the spatial

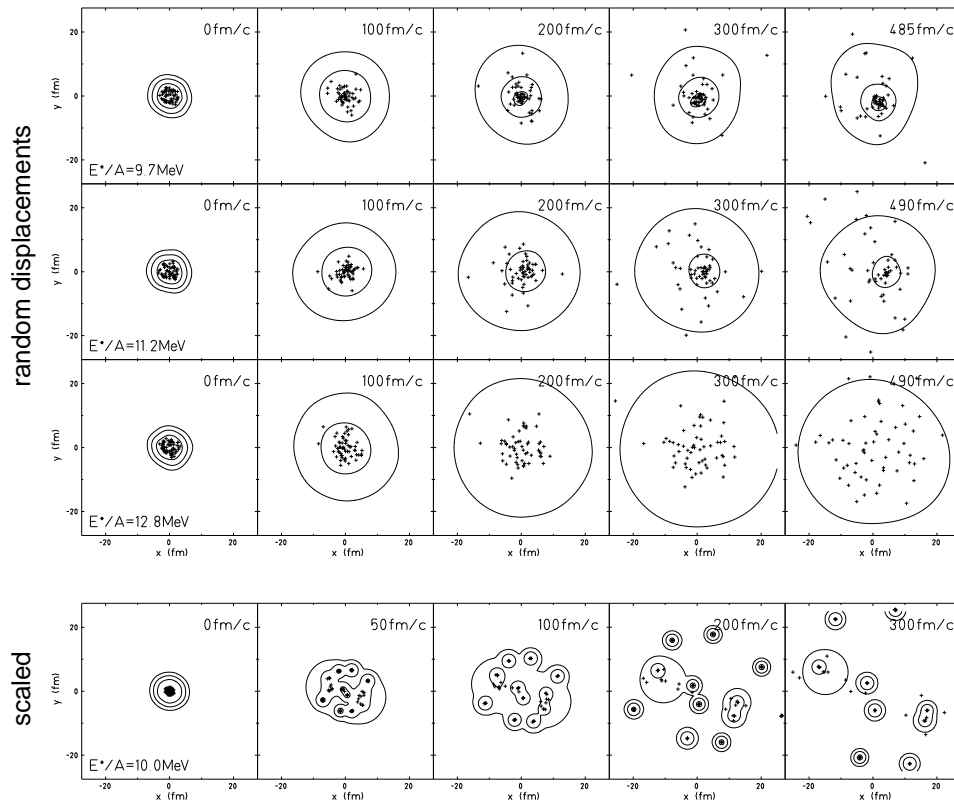


Figure 2: Density plots of the decay of excited ^{56}Fe nuclei.

correlations in the cluster structure of the ground state. The three different excitation energies are achieved by randomly displacing the centroids of the gaussian from their ground state positions but keeping the density at normal values. In all cases the nuclei show first an expansion caused by the increased pressure. If the excitation energy or the pressure is not too high (first two rows) a contraction follows in the center where the mean field is still strong enough to hold together a hot fragment which finally deexcites by particle evaporation. Typically between 11 and 12 A MeV excitation the nuclei vapourize into individual nucleons.

In the last row the excitation energy of 10 A MeV is created by scaling down the distances between the centroids of the gaussians. In addition small random displacements are applied. These excitations do not destroy the spatial correlations between the nucleons and multifragmentation into different clusters is observed.

The conclusion is, that in FMD initial correlations are important to form clusters. There is not enough time during the decay and expansion of a randomly excited nuclear system to build up the many-body correlations needed to form a rather cold fragment. Either the fragments originate from cool junks of the initial system or we observe evaporation residues.

3 Unitary Correlator Operator Method

To avoid the above demonstrated ambiguities and to gain predictive power we want to start from realistic nucleon-nucleon potentials. There is however the old problem that realistic interactions, which reproduce the scattering and deuteron data, feature a strong short range repulsion and also tensor, spin-orbit and momentum-dependent parts. The numerically convenient single determinant is only appropriate if the system is dominated by a mean field but it is not sufficient to represent the two-body correlations induced by the short ranged repulsion and the tensor interaction. Since we do dynamical calculations with many time steps a G-matrix method with a Pauli-operator which depends on the actual state and therefore on time is not advisable.

Our approach to treat these correlations in a simpler fashion is similar to the Jastrow method but in order to avoid complications with a time-dependent norm in dynamical calculations we construct a unitary correlation operator which does not depend on the actual time evolution. This conserves the norm of the correlated state and also allows to apply the correlation operator in a state-independent way to operators, resulting in correlated operators.

In a first step we developed the Unitary Correlation Operator Method (UCOM) [4, 9, 6] to treat the strong short-range repulsion of the realistic interactions. The correlator \tilde{C} shifts the relative wave function of each pair of particles out of the

repulsive region of the interaction. In two-body space it is defined with the hermitian two-body operator \tilde{S} which acts on the relative coordinate \vec{x} in the following way:

$$\langle \vec{X}, \vec{x} | \tilde{C} | \Phi \rangle = \langle \vec{X}, \vec{x} | e^{-i\tilde{S}} | \Phi \rangle = \exp \left\{ -\frac{1}{2}s'(x) - \frac{s(x)}{x} - s(x)\frac{\partial}{\partial x} \right\} \langle \vec{X}, \vec{x} | \Phi \rangle. \quad (6)$$

$s(x)$ determines the amount by which the particles are shifted away from each other. Using correlation functions R_+ and R_- defined by

$$\int_x^{R_-(x)} \frac{dt}{s(t)} = -1, \quad \int_x^{R_+(x)} \frac{dt}{s(t)} = +1. \quad (7)$$

We can write the correlated wave function in terms of a coordinate transformation as

$$\langle \vec{X}, \vec{x} | \tilde{C} | \Phi \rangle = \frac{R_-(x)\sqrt{R'_-(x)}}{x} \langle \vec{X}, \frac{\vec{x}}{R_-(x)} | \Phi \rangle. \quad (8)$$

If we apply the correlation operator to operators we get the corresponding correlated operators which act between uncorrelated states.

$$\langle \hat{Q} | \tilde{B} | \hat{Q} \rangle = \langle Q | \tilde{C}^\dagger \tilde{B} \tilde{C} | Q \rangle = \langle Q | \hat{B} | Q \rangle, \quad \hat{B} = \tilde{C}^\dagger B \tilde{C} \quad (9)$$

Of special interest is the correlated Hamilton operator \hat{H} . Besides the transformed two-body potential $V(R_+)$ we get two-body interaction parts from the correlated kinetic energy which has momentum-dependent and potential-like contributions.

Three-body and higher contributions from the correlated operators can be neglected if the correlation volume times the density is small enough so that the probability to find three or more particles simultaneously within the range of the strong repulsion is small.

As a test of the method we applied it to the Afnan-Tang S3M potential. This pure central potential has been used as a benchmark for many-particle methods. In fig. 3 the results of FMD calculations with the Unitary Correlation Operator Method are shown. The agreement with other, numerically much more expensive, methods is striking. The kinetic energy of the correlated state increases in comparison to the uncorrelated one but this is overcompensated by the gain in potential energy. It is amazing to see how accurately the large positive and large negative corrections from the correlations add up to the correct binding energy.

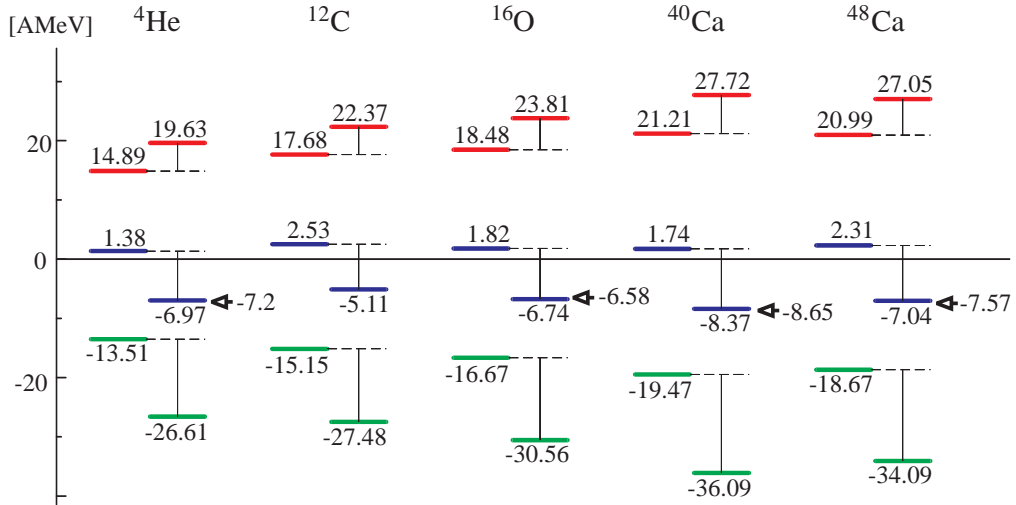


Figure 3: FMD calculations using the ATS 3M potential. For each nucleus expectation values of kinetic (top), potential (bottom) and binding (middle) energy per nucleon are shown. The left hand columns display the values for the uncorrelated and the right hand columns for the correlated states. The arrows indicate results of other methods, Yakubovskii (⁴He), FHNC (¹⁶O) and CBF (⁴⁰Ca and ⁴⁸Ca). References in [4].

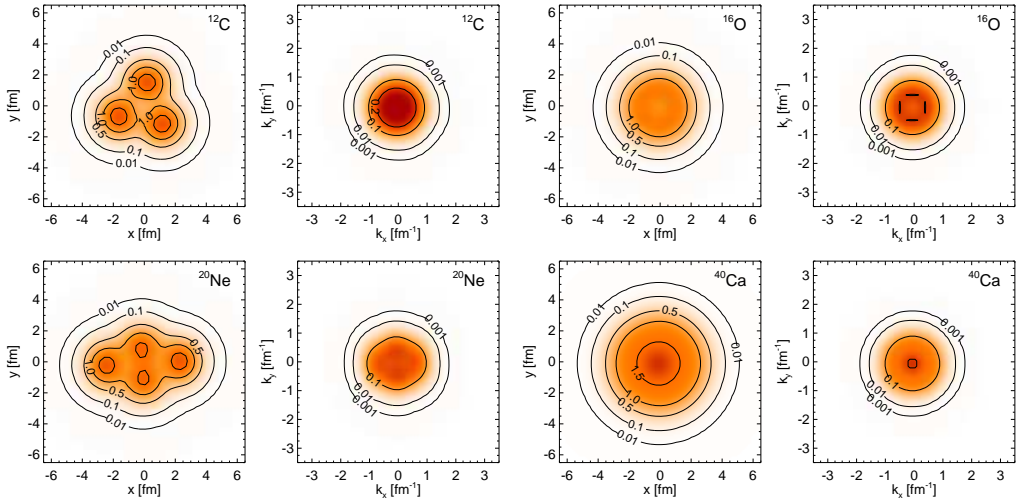


Figure 4: FMD ground states with the ATS 3M potential. Plotted are cuts of the nucleon density in coordinate and momentum space.

Particularly interesting is the FMD result for ^{12}C . Other methods have great difficulties to describe the intrinsic structure of this nucleus well. The FMD result is shown in fig. 4, where cuts of the nucleon density in coordinate and momentum space are plotted. One can clearly see that the FMD trial states with gaussians can describe both intrinsically deformed states like ^{12}C or ^{20}Ne and closed shell states like ^{16}O or ^{40}Ca .

One should, however, keep in mind that in real nuclei a major part of the binding originates from the tensor interaction which induces correlations between the spin of two particles and the direction of their relative distance vector. We are developing a unitary correlator for these tensor correlations but the correlated hamiltonian is of a rather complicated form and results are not available yet.

4 Configuration Mixing

If one wants to address questions of nuclear structure in the FMD environment more refined trial states are necessary and possible. The parameterization of the one-particle state can be improved by using a superposition of several gaussians. This strategy promises to be useful for the description of halo-nuclei with their far out reaching exponential tail in the nucleon density [6].

On the other hand superpositions of Slater determinants can lead to a better description of medium and long ranged many-particle correlations. To demonstrate this approach we present an improved treatment of the ^{12}C ground state. As shown in the last section the FMD ground state is given by an intrinsically deformed single Slater determinant which of course lacks the symmetries of the real ^{12}C state regarding parity and angular momentum. As an alternative to the projection on the right quantum numbers we perform a configuration mixing calculation in a set of randomly rotated FMD states. Formally this leads to a generalized eigenvalue problem where the Hamilton operator is represented in a nonorthogonal set of FMD states $\{|\hat{Q}^i\rangle\}$:

$$\sum_j \langle \hat{Q}^i | \hat{H} | \hat{Q}^j \rangle c_j^\alpha = E^\alpha \sum_j \langle \hat{Q}^i | \hat{Q}^j \rangle c_j^\alpha. \quad (10)$$

The energies of the lowest eigenstates of such a configuration mixing calculation are shown in fig. 5 as a function of the number of basis states. With increasing number of basis states the lowest states become better and better eigenstates of parity and angular momentum and the rotational bands emerge. One can also observe a rather large increase in binding energy of about 12 MeV for the ground state.

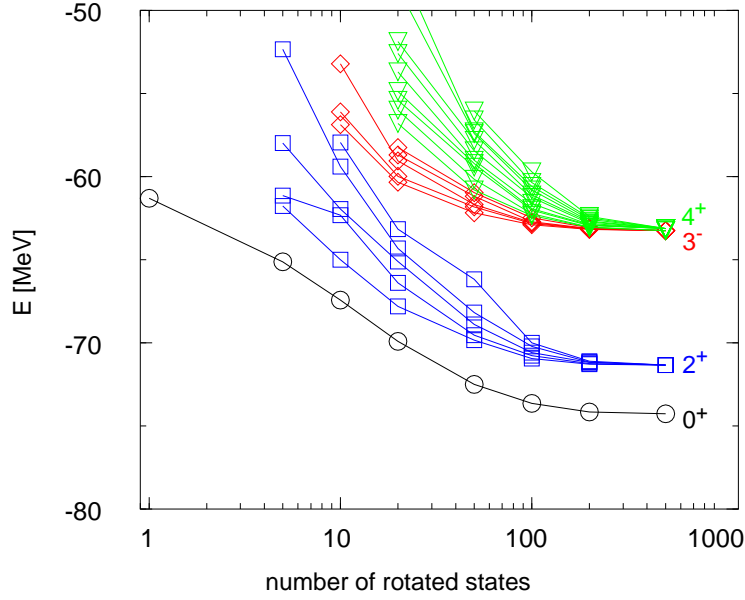


Figure 5: Results of configuration mixing calculations – plotted are the energies of the lowest states as a function of the basis dimension.

5 Some Ideas about Quantum Branching

Since the antisymmetrized products of gaussians form an overcomplete basis set in Fock space any many-body state, also the exact solution of the Schrödinger equation, can in principle be represented by a superposition of FMD states. The configuration mixing calculation for ^{12}C in the previous section shows for example the ground state as a superposition of many Slater determinants. In a dynamical calculation we can for numerical reasons only follow the evolution of a single component. But like in the stationary situation this component mixes via off-diagonal matrix elements of the hamiltonian with other determinants during the time evolution. Many models, like AMD [8, 7] or QMD [1] simulate these quantum branchings by means of random collision terms.

A more refined treatment of this effect should be possible by allowing the FMD state $|Q(t)\rangle$ to have a certain possibility to jump to another FMD state $|Q'(t)\rangle$. This branching to another trajectory should be determined by the perturbation operator

$$i \sum_{\mathbf{v}} \dot{q}_{\mathbf{v}} \frac{\partial}{\partial q_{\mathbf{v}}} - \tilde{H} \quad (11)$$

which describes the difference between the FMD and the exact time-evolution. Open problems are the conservation laws and the approximation needed to come

from perturbative transition amplitudes to transition probabilities. If the system is in an energy regime with high level density statistical arguments may be employed.

Quantum branching is probably not only needed in multifragmentation to jump from a situation with wide wave packets to cluster states, but also in general to allow for example crossing of potential barriers which exist in the highly restricted phase space of the parameters but can be tunneled in reality.

Another example is the breaking of symmetries. The exact final state possesses the dynamically conserved symmetries of the initial state simply by a superposition of a channel and its counterpart. An illustrative example is the left-right mirror symmetry of the $^{40}\text{Ca}+^{40}\text{Ca}$ reaction. After the collision the measured channels are of course not symmetric, only the superposition of all channels has the proper symmetry. When in the approximate scheme only a single state, which has initially the mirror symmetry, is evolved in time, it will conserve this symmetry in a too restricted way. During the evolution the symmetry should be broken by quantum branching such that with equal probability each final channel and its mirrored counterpart can be reached.

References

- [1] Jörg Aichelin, Regina Nebauer, in *these proceedings*
- [2] Hans Feldmeier, Nucl. Phys. **A515** (1990) 147
- [3] Hans Feldmeier, Konrad Bieler, Jürgen Schnack, Nucl. Phys. **A586** (1995) 493
- [4] Hans Feldmeier, Thomas Neff, Robert Roth, Jürgen Schnack, Nucl. Phys. **A632** (1998) 61
- [5] Hans Feldmeier, Jürgen Schnack, Prog. Part. Nucl. Phys. **39** (1997) 393
- [6] Thomas Neff, *Fermionische Molekulardynamik mit Konfigurationsmischungen und realistischen Wechselwirkungen*, Master's thesis, TU Darmstadt (1998)
- [7] Akira Ono, Hisashi Horiuchi, in *these proceedings*
- [8] Akira Ono, Hisashi Horiuchi, Phys. Rev. **C53** (1996) 2958
- [9] Robert Roth, *Die Methode der unitären Korrelatoren*, Master's thesis, TH Darmstadt (1997)